Mineralogical characterization of paulingite from Vinaricka Hora, Czech Republic

C. L. Lengauer, G. Giester and E. Tillmanns

Institut für Mineralogie und Kristallographie, Universität Wien - Geozentrum, Althanstrasse 14,
A-1090 Wien, Austria

Abstract

A sample of the zeolite paulingite from the locality Vinaricka Hora was investigated by means of chemical, thermal, powder and single crystal X-ray methods. The fully transparent, colourless to pale yellow crystals exhibit the form $\{110\}$ and occur together with phillipsite. The chemical composition is $(Ca_{2.57}K_{2.28}Ba_{1.39}Na_{0.38})(Al_{11.55}Si_{30.59}O_{84}) \cdot 27H_2O$, $Z = 16$ with minor amounts of Mg (<0.05), Sr (<0.13), Mn (<0.01), and Fe (<0.04). The chemical differences from previously described paulingites are a high Ba-content, a lower Si/(Al+Fe) ratio of 2.64, and a reduced water-content. The calculated density is 2.098 g cm^{-3}, and the observed refractive index is 1.482(2). The dehydration behaviour is characterized by a main weight loss from 24−190°C (−11.2 wt.%, $\cong$ 21H$_2$O) and a minor weight loss from 190−390°C (−3.1 wt.%, $\cong$ 6H$_2$O). The rehydration capability was proven up to 150°C. The dehydration process during the main weight loss is accompanied by a reduction of the cell volume of 11%. The refined lattice parameters of the X-ray powder data are $a = 35.1231(5)$ Å and $a = 33.7485(8)$ Å of an untreated and a dehydrated sample, respectively. A breakdown of the paulingite structure can be observed while the remaining water content decomposes. The single crystal X-ray refinement of this chemically different sample material derived three main cation positions, which are inside a so called paulingite or π-cage (Ca), between 8-rings of neighbouring π-cages (Ba), and in the centre of the non-planar 8-rings of the γ-cage (K). Further partially occupied cation positions (Ca,Na) were located in the planar 8-rings of the α- and γ-cages. No positions within the double 8-membered rings were detected. The water is localized around the main cation positions and in three clusters of partially occupied sites.

KEYWORDS: paulingite, zeolite, structure refinement, Vinaricka Hora, Czech Republic.

Introduction

PAULINGITE, a rare zeolite mineral, was first described by Kamb and Oke (1960) from vesicles in the Tertiary, augite-bearing basaltic rocks at the Rock Island Dam, Washington DC, famous for their zeolite parageneses (Speckels, 1991). The first suggestion of the mineral name paulingite, by Efremov (1951), however, was proposed for an intermediate member of the serpentine mineral group never approved by the CNMMN. Apart from the type locality, three further occurrences of paulingite are known from Riggins in Idaho County, Ritter in Grant County, and Chase Creek in British Columbia (Tschernich and Wise, 1982). In Europe, paulingite was found among the zeolites of the Irish Giant's Causeway (Nawaz, 1988), and reported from two German 'zeolite-localities' near Höwenegg (Walenta et al., 1981) and Vogelsberg

(Hentschel, 1986). An additional paulingite locality was described briefly by Hlouek et al. (1988) from the Vinaricka Hora, former CSFR.

The mineralogical information about paulingite is based mainly on the description of Kamb and Oke (1960) and the mineralogical comparison of the four North American localities by Tschernich and Wise (1982). They observed a very large cubic cell with $a \approx 35.1$ Å, and a typical dodecahedral crystal form $\{110\}$ as characteristic of paulingite. The chemistry was summarized with a Si/Al ratio of ~3.0, a BaO range of 0.5−4.1 wt.%, a water content of 18.5 wt.%, and a general formula $(Ca_1,K_2,Ba_1,Na_2)_5$ $(Al_{10}Si_{32}O_{84}) \cdot 34−44H_2O$ ($Z = 16$). A compilation of the mineralogy on paulingite is given in Gottardi and Galli (1985) and in Tschernich (1992).

The crystal structure of paulingite was determined by Gordon et al. (1966) using crystals from the type locality. They confirmed the space group $Im3m$,
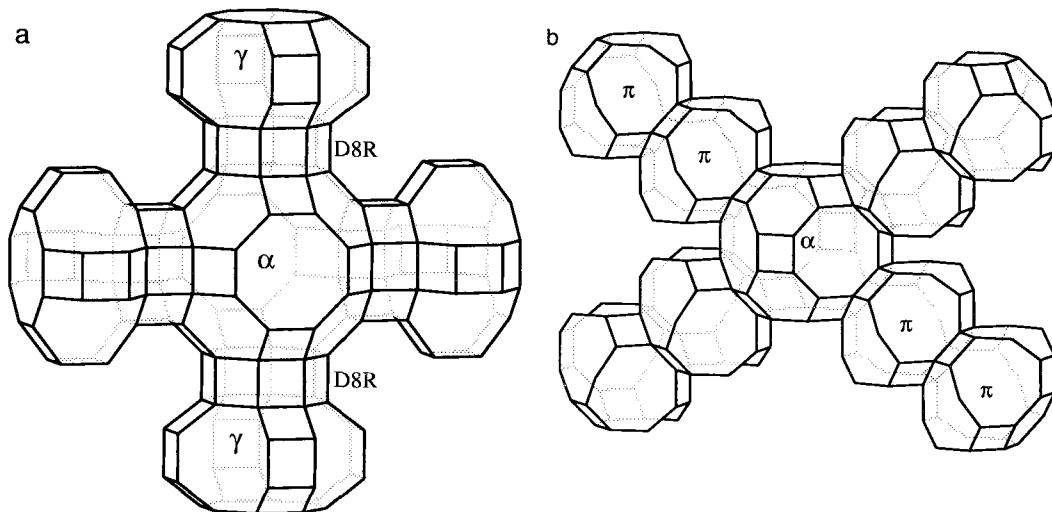
FIG. 1. Three-dimensional slices (a) of the -γ-D8R-α-D8R-γ- main channel system parallel the plane (½,0,0) with the dynamic diameter of ~4.26 Å, and (b) of the -π-π-α-π-π- minor diagonal channel system parallel the plane (110) with the dynamic diameter of ~2.50 Å. The π-cage can be derived from the levyn-cage with a replacement of the 6-ring plus the neighbouring 4-ring by a single 8-ring.

proposed by Kamb and Oke (1960), and gave a description of the complex paulingite framework topology designated with the IZA-code PAU (Meier *et al.*, 1996). The accuracy of their structure refinement (final R_F = 14%), however, did not allow a crystallochemical assignment of the non-framework components to the locations within the zeolite pore system.

The tetrahedral framework topology of paulingite is characterized by a connecting double 8-ring (D8R), which links alternatively the building unit of a truncated cuboctahedron (α-cage) with a fourfold analogue of the threefold gmelinite-cage, the γ-cage. These two building units can also be observed singly in the KFI- topology of the synthetic zeolite ZK-5 (Meier and Kokotailo, 1965). Using these three polyhedral units, the main pore system of paulingite can be described by two parallel, but independent sets of a three-dimensional channel systems oriented along the principal axes and shifted ½,½,½ against each other. This channel arrangement is similar to ZK-5, however, the paulingite cage sequence along the main channels can be given as -α-D8R-γ-D8R-γ-D8R-α- (Fig. 1a), whereas in ZK-5 the succession -α-γ-α- can be observed. In the framework of pahasapaite (RHO-topology), on the other hand, the sequence -α-D8R-α- is established (Rouse *et al.* 1989). The two channel sets are connected via semicircular, 'horseshoe-like' bands of five 4-rings attached outside of the nonplanar 8-rings of the

γ-cages (cf. Fig. 5c). Along the threefold axis of paulingite a second type of a channel system exists (Fig. 1b), which is built up by the α-cage and a modified form of the levyne-cage only observed in the paulingite topology (π-cage). These units are combined via single 6-rings (S6R) resulting in the sequence -α-π-π-α-.

The complexity of the framework has given rise to several different topological descriptions based on a relationship to gismondine (Andersson and Fälth, 1983), on four-leafed clover like double 24-rings (Gottardi and Galli, 1985), on the linkage of the α-cages (Hawthorne and Smith, 1986), or on a generalized characterization of the cages using a classification of face symbols (Smith, 1989). The synthetic aluminosilicate ECR-18, proposed as isostructural with the paulingite topology, is documented by Vaughan and Strohmaier (1987), who obtained sodium-zeolites with $a = 35 \pm 1$ Å, and a Si/Al-ratio from 6 to 20.

The sample material of the present work was supplied by the Czech mineralogist F. Cech, in order to clarify the chemistry of paulingite from Vinarická Hora. A preliminary chemical inspection yielded a lower Si/Al-ratio and a higher Ba-content as compared to the data published before, thus encouraging a complete mineralogical investigation of this material. Besides the crystallochemical characterization of the non-framework components, a contribution to the almost unknown structural

behaviour of paulingite during the dehydration process is presented.

Occurrence and paragenesis

The paulingite under investigation originates from the hill of Vinarická Hora, an isolated complex of augite-bearing nephelinite in the north of Kladno (Katzer, 1892), which belongs to the Miocene phase of a Tertiary volcanism within the Mesozoic area of the Bohemian Massif (Suk, 1984). Inside vesicles of these volcanic rocks paulingite occurs in association with water-clear crystals of phillipsite, both imbedded in, or overgrown by a carbonate layer. The fully transparent, colourless to pale yellow, idiomorphic crystals exhibit solely the crystallographic form {110} reaching sizes up to 2 mm in diameter. Intergrowths of several crystals and cracks are abundant and often only observable under the polarizing microscope. The paulingite crystals are sometimes overgrown by phillipsite, which commonly exhibits Morvenite-type twinning. The sample material is preserved in the systematic collection of the Institut für Mineralogie und Kristallographie, Universität Wien, under the catalogue number 8J/27-050#1.

Physical and chemical properties

For optical investigation, a spindle-stage was used. Zoning due to growth conditions or chemical inhomogenities was not observed. The refractive index of 1.482(2) using Na_D-light ($\lambda = 598.3$ nm) is in the higher range of the reported values (1.472–1.484, Tschernich, 1992). The calculated refractive index using the Gladstone-Dale relationship is significantly lower ($n_c = 1.46$). According to the work of Mandarino (1981) the refractive energy of molecular water is the dominant and positively correlated parameter influencing the refractive index of zeolitic compounds. The Si/Al-ratio at the tetrahedral sites of the framework and its charge compensation by alkaline and earth alkaline elements within the zeolite pore system can be expected to be only of minor influence. The experimental uncertainty of the interaction between the zeolite and the immersion liquid, however, lowers the significance of absolute refractive index values.

The water content was studied by a thermogravimetric analysis (TGA) of 3.12 mg hand picked and fine grained paulingite with a Mettler M3 microbalance under nitrogen atmosphere up to 800°C with a heating rate of 5°C min^{-1} (Fig. 2). To avoid a
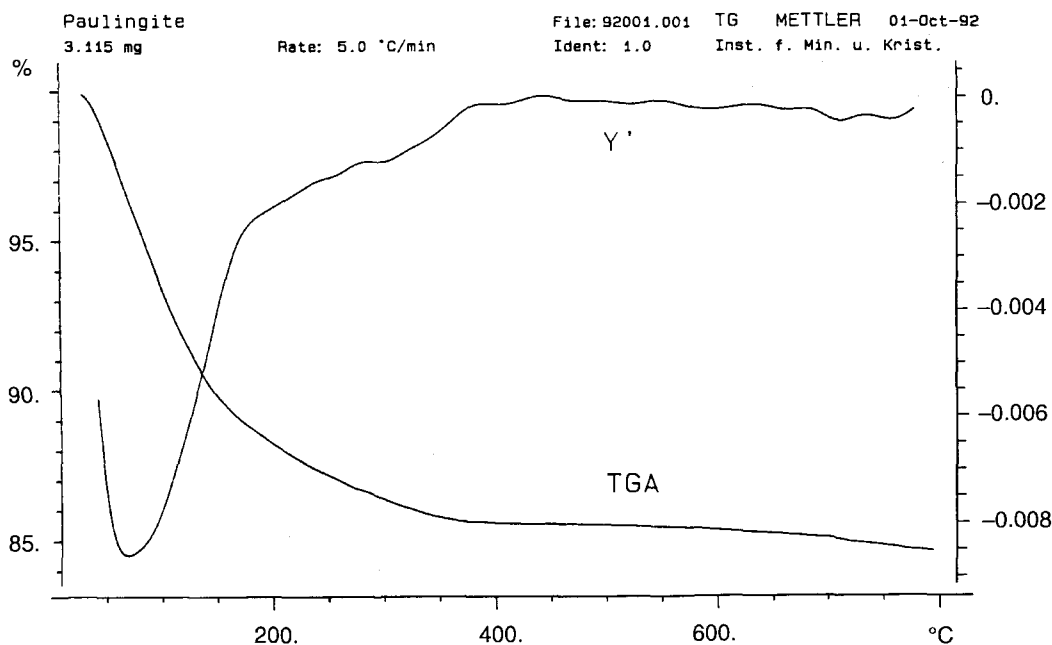
FIG. 2. The thermogravimetric analysis (5°C min^{-1}) of paulingite from the Vinarická Hora with weight loss (TG) in wt.% (left axis) and its derivative (Y') in wt.% min^{-1} (right axis).

weight loss at the initial stage of the measurement, a starting temperature of 24°C was chosen, and the equilibration time under dry nitrogen was reduced to 30 s. The release of H_2O is noted to have already begun at slightly above room temperature with a maximum of the first derivative at ~70°C (24−190°C: −11.2 wt.%), a further, poorly resolved maximum is observed at 310°C (190−390°C: −3.1 wt.%).

Considering the different heating rate of 20°C min^{-1} used by Gottardi and Galli (1985) for the TGA-analysis of the paulingite from Ritter, these weight losses correspond to their first and third maxima at 100°C (−9 wt.%) and 380°C (−3 wt.%), respectively. For their second shown maximum at 200°C (−5.5 wt.%) no equivalent behaviour was observed in our investigation. The difference in the dehydration processes is likely to be caused by the actual particle size of the examination, i.e. desorption properties *vs* blocking of the pore system by structural faults. This is supported by the observation of Vaughan and Strohmaier (1987), who found a continuous water decomposition of 15.5 wt.% from room temperature to 300°C for their synthetic powder with crystal diameters $\leqslant$ 0.5 μm. In this context it is interesting to note that intense cracking under the evacuated conditions of EMP or SEM measurements has frequently been described, a feature also observed during our microprobe analysis.

Assuming that the whole weight loss up to 390°C (−14.3 wt.%) is attributed to H_2O, an overall water content of ~$27H_2O$ per formula unit can be calculated, with ~$21H_2O$ in the range of 24−190°C and ~$6H_2O$ in the range of 190−390°C. Despite the fact that our refractive index is high, compared to literature values, our water content is significantly lower than the data given in Tschernich and Wise (1982) or Gottardi and Galli (1985) for the Ritter paulingite (~$35H_2O$), and the value of Kamb and Oke (1960) for the type material (~$44H_2O$). Intense resorption and dehydration processes even at room temperature obviously cause these inconsistencies. The rehydration capability was proven by TGA measurement cycles to be given up to 150°C, which corresponds almost exactly with the first main weight loss.

The empirical formula of paulingite, ideally $((M^{1+})_2, M^{2+})_5(Al_{10}Si_{32}O_{84}) \cdot nH_2O$ with $Z = 16$, was determined by microprobe analysis of four crystals to be $(Ca_{2.57}K_{2.28}Ba_{1.39}Na_{0.38})$ $(Al_{11.55}Si_{30.59}O_{84})$ $\cdot 27H_2O$ (Table 1). Minor amounts [p.f.u.] of Mg ($\leqslant 0.05$), Sr ($\leqslant 0.13$), Mn ($\leqslant 0.01$), and Fe ($\leqslant 0.04$) are detected. The observed Si/(Al+Fe) ratio of 2.64 is significantly lower than the range of 2.9−3.3 reported by Tschernich and Wise (1982) and the value of 3.4 given by Gordon *et al.* (1966). The non framework chemistry differs from the given range

(Tschernich, 1992: Ca 1.9−3.7, K 2.7−4.7, Ba 0.1−0.8, Na 0.4−1.0 p.f.u.) due to the significantly higher Ba content, compensated mainly by the low K-content. The charge error defined by Tschernich and Wise (1982) and Gottardi and Galli (1985) is 5.7% and 6.0%, respectively. No chemical zoning was observed in the four investigated crystals. The calculated density based on the chemical formula (d_x = 2.089 g cm^{-3}) is very close to the observed one (d_o = 2.085) of Tschernich and Wise (1982).

Ambient and non-ambient X-ray powder characterization

Several hand-picked crystals of paulingite were ground smooth and one portion of the powder was kept at room conditions, and a second dehydrated under a vacuum of 10^{-7} mbar (12 h) and heated to 50°C for the last 3 h. Both samples were sealed in glass capillaries (θ = 0.3 mm). The X-ray powder patterns were collected on a STOE STADIP transmission diffractometer system using Debye-Scherrer geometry and a PSD detector system. Further details of the powder measurement are compiled in Table 2, the observed powder patterns are presented in Fig. 3, and the respective d_{hkl}-I_{hkl} listings are tabulated in Tables 3 and 4.

The comparison of the simulated powder pattern of Treacy *et al.* (1996), which is based on the data of Gordon *et al.* (1966), with our data of the untreated sample, reveals a significant lowering of the intensities in the angular region below 20°2θ, which can be attributed mainly to the presence of low ordering of the water molecules within the pore system. In order to discard an absorption effect, a further measurement up to 40°2θ using a different capillary dimension (θ = 0.1 mm) was performed, which reveals the same intensity distribution. In the range $\leqslant$ 10°2θ three peaks at d = 24.80 (110), 17.55 (200), and 14.30 Å (211) were detected, not given in the data of the JCPDS-File (No. 39-1378). The refined cell parameter a = 35.1231(5) Å of the untreated sample is larger than those given by Tschernich and Wise (1982): 35.049−35.093 Å.

The powder pattern of the dehydrated sample is characterized by the expected enlargement of the low angular peak intensities, a huge increase of the (330) reflection, and a slight decrease of the sample crystallinity. The refinement of the cell parameter yielded a heretofore unknown, unusually low value of a = 33.7485(8) Å, which corresponds to a shrinkage of the cell volume of 11%. No indication of a change in space group symmetry was observed.

For additional data on the thermal stability of paulingite, a third powder sample was prepared as a thin film and investigated on a HUBER HT-Guinier camera using Cu-$K_{\alpha 1}$ radiation, and steps of 20°C,

TABLE 1. Chemical analyses of paulingite from Vinarická Hora

	Electron microprobe analyses [wt.%]								Cell contents p.f.u. normalized to 84 oxygens (Z = 16)				
	A		B		C		D			A	B	C	D	$\bar{x}$
SiO_2	55.54	53.59	55.65	53.55	56.96	55.01	56.22	54.01	Si	30.44	30.46	30.84	30.62	30.59
Al_2O_3	18.14	17.50	18.09	17.41	17.72	17.11	17.82	17.12	Al	11.72	11.68	11.32	11.44	11.55
Fe_2O_3	0.03	0.03	0.06	0.06	0.08	0.08	0.10	0.09	Fe	0.01	0.02	0.04	0.04	0.03
K_2O	3.29	3.17	3.25	3.13	3.19	3.08	3.37	3.24	K	2.30	2.27	2.21	2.34	2.28
CaO	4.40	4.25	4.41	4.24	4.36	4.21	4.38	4.21	Ca	2.59	2.58	2.53	2.56	2.57
BaO	6.60	6.36	6.78	6.52	6.18	5.97	6.47	6.22	Ba	1.42	1.45	1.31	1.38	1.39
Na_2O	0.35	0.36	0.34	0.33	0.32	0.31	0.40	0.38	Na	0.40	0.37	0.34	0.42	0.38
SrO	0.40	0.39	0.39	0.37	0.37	0.36	0.36	0.35	Sr	0.13	0.12	0.11	0.12	0.12
MgO	0.05	0.05	0.07	0.07	0.05	0.05	0.06	0.06	Mg	0.04	0.05	<0.01	0.05	0.04
MnO	0.01	0.01	0.02	0.02	0.03	0.03	0.03	0.03	Mn	<0.01	<0.01	0.01	0.01	0.01
$H_2O_{(TGA)}$	–	14.3	–	14.3	–	14.3	–	14.3	H_2O	27.2	27.2	27.0	27.1	27.1
Σ wt.%	88.81	100.0	89.06	100.0	88.74	100.0	89.21	100.0	Si/Al	2.60	2.61	2.72	2.68	2.64
									$\Sigma T^{(i)}$	42.17	42.16	42.20	42.10	42.17
									$\Delta charge^{(ii)}$	0.05	0.05	0.06	0.03	0.05
Mean of	n = 6		n = 11		n = 14		n = 12							

Microprobe measurement conditions: 15 kV, 8–9 nA, focus θ 10 μm, time/element 8–10 sec. Used standards: jadeite $Na_{11.13}Al_{13.40}Si_{27.87}O_{47.60}$, 'SrCuSi4' $Cu_{15.00}Sr_{20.69}Si_{26.53}O_{37.78}$, pyrope $Mg_{18.09}Al_{13.39}Si_{20.90}O_{47.62}$, andradite $Ca_{23.66}Fe_{21.98}Si_{16.58}O_{37.78}$, spessartine $Mn_{33.29}Al_{10.90}Si_{17.03}O_{38.78}$, Ba-glass $Ba_{50.21}Si_{20.54}O_{29.25}$, K-glass $K_{6.30}Ca_{12.00}Mg_{7.28}Al_{4.35}Si_{25.87}O_{44.20}$.

TGA measurement conditions: 24–800°C, 5°C min^{-1}, 3.115 mg, dry N_2 (9.5) atmosphere.

(i) $\Sigma T = Si + Al + Fe$, (ii) $\Delta charge = [(Al+Fe) - \Sigma charge_{(K, Ca, Ba, Na, Sr, Mg, Mn)}]/(Al+Fe)$ after Tschernich and Wise (1982).

TABLE 2. Summary of measurement conditions, crystallographic parameters, and physical properties of paulingite from Vinaricka Hora

X-ray powder data collection and refinement

Sample preparation	sealed glass capillary, θ 0.3 mm, 3 rotations/sec	
Radiation	Cu-$K_{\alpha 1}$ (Ge - monochromator)	
Calibration	Si$_{(111)}$ to 28.443°2θ, externally	
Effective step size [°2θ]	0.2	
Detector resolution [°2θ]	0.02	
2θ-range, total time [h]	2.0−38.0	9.0
	37.0−67.0	12.5
	66.0−87.0	10.5
	86.0−95.0	5.3

	natural	dehydrated
a_o[i]	35.1231(5) Å	33.7485(8) Å
V_o	4.3329 × 10^4 Å^3	3.8438 × 10^4 Å^3
$F_{(30)}$[ii]	217.0 (0.004, 36)	110.3 (0.008, 34)
$F_{(151)}$	110.6 (0.006, 244)	63.0 (0.100, 244)

X-ray single crystal data collection and refinement

Z	16	Space group	*Im3m*
μm(Mo-K_α)	1.288 cm^{-1}	Radiation	Mo-K_α (graphite monochromator)
sinθ/λ_{max}	0.705 Å^{-1}	$h\,k\,l$ $_{min/max}$	−34/49; −34/35; 0/45
$R1$	0.199	Measured reflections	20799
w$R2$	0.168	Unique reflections	5900
R internal	0.062	Reflections $F_o > 4\sigma\,F_o$	2221
$R1 > 4\sigma$	0.069	Variable parameters	294

Physical parameters

	Natural	Dehydrated
d_x	2.098	2.017
n_o	1.482(2)	n.d.
n_c[iii]	1.42	1.31

[i]refined lattice parameters from powder data using the algorithm of Appleman and Evans (1973), [ii]figure of merit as given by Smith and Snyder (1979), [iii]calculated refractive index after Mandarino (1981)

3 h exposure time each, in the range 30−350°C. As can be derived from the change of the paulingite cell parameter (Fig. 4), the water decomposition corresponding to the first weight loss of the TGA measurement causes a steep decrease of the cell parameter associated with peak broadening to the value determined from the dehydrated sample. In the temperature range from 150−250°C the structure exhibits a moderate decrease of the unit cell. Above 250°C, however, the breakdown of the structure is documented by a starting of a further steep cell parameter reduction accompanied by peak broadening. This behaviour corresponds to the second and final weight loss with its weak maximum at 310°C.

Single crystal structure refinement

A selected fragment of a rhombic-dodecahedron with a maximal dimension of ~0.5 mm in diameter was initially investigated by Weissenberg (Cu-K_α) and Buerger (Mo-K_α) film methods to exclude intergrowths and to confirm the reported space group *Im3m* (No. 229). The single crystal data were collected on a Stoe-AED2 four-circle diffractometer. Details of the intensity measurements and refinement procedures as well as crystal data are compiled in Table 2. The X-ray intensities were corrected for Lorentz and polarization effects as well as for absorption by evaluation of ψ-scans.
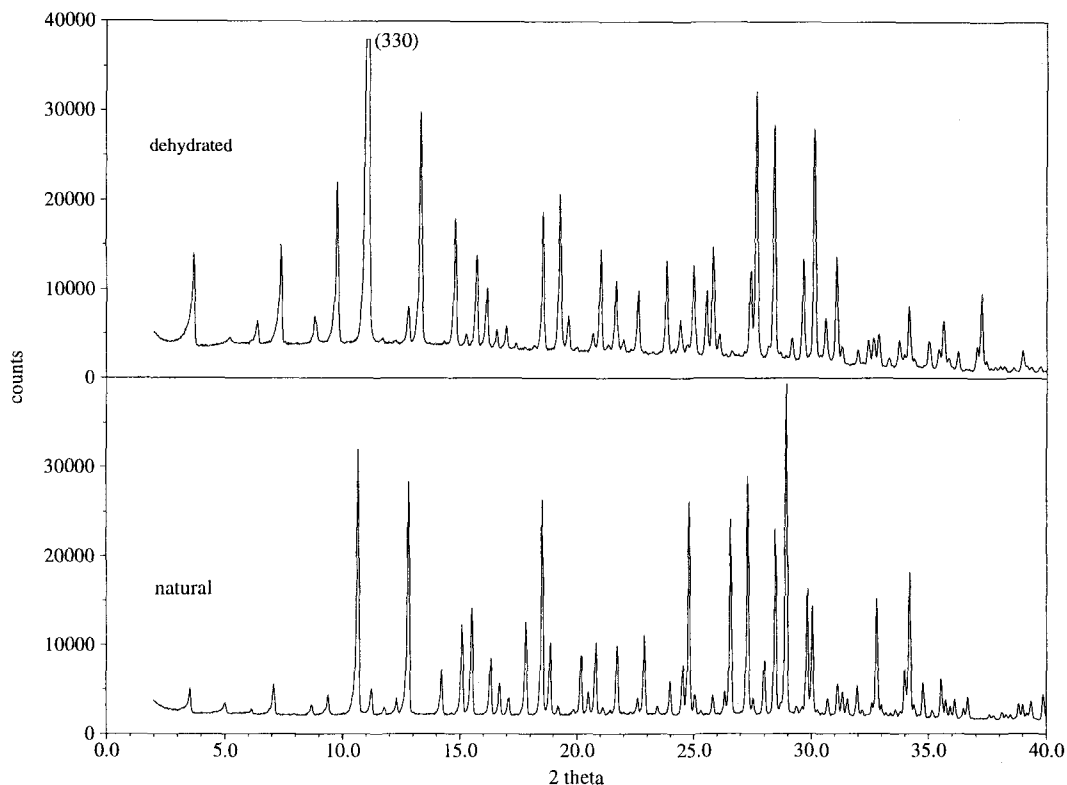
FIG. 3. The observed powder diffraction patterns of the untreated paulingite from the Vinarická Hora and the dehydrated sample. For a better comparison, the (330) reflection of the dehydrated paulingite is clipped at a third of its measured intensity.

The structure refinement was started with the atomic coordinates of the framework as given by Gordon *et al.* (1966). The Si/Al ratio of all framework cations was fixed according to the chemistry. By difference Fourier maps, a suite of maxima within the channels and cages was localized, confirming the model proposed by Gordon *et al.* (1966). Additional maxima were also observed, some of which could be attributed to further cations or water molecules, even if not fully occupied. Taking into account the observed chemical formula and the results of the difference Fourier synthesis, the occupation of the cation- and water-sites was obtained using constraints on displacement and site occupation factors. The final atomic parameters of the framework and of the pore filling, refined by least-squares techniques on F^2 (SHELXL-96, Sheldrick 1996), are given in Tables 5 and 6, respectively. Relevant interatomic distances and angles are listed in Table 7. The proposed structure model accounts for about 99 of the 106 cations and 390 of the 432 water molecules of the channels and

cages as compared with the results of the chemical analyses. The residual electron densities in the final difference Fourier analysis are $\leqslant 1.3$ and $\geqslant -0.6$ eÅ^{-3}.

Encouraged by the results of the X-ray powder investigations different experimental approaches were used in order to get a dehydrated crystal specimen suitable for structure refinement. Unfortunately all attempts failed, because of the intense cracking as a result of the volume change. The only fact, which can be derived from two preliminary single crystal data collections, is the confirmation of the space group symmetry *Im3m* as it was indicated by the powder measurement before.

The framework

The mean interatomic distances (Table 7) derived from the refined framework coordinates (Table 5) vary between 1.63 Å (T5) and 1.64 Å (T6) and gave no indication of a Si/Al ordering over the tetrahedral positions. The results are in a good accordance with

TABLE 3. X-ray powder diffraction data of untreatd paulingite from Vinarická Hora

d_{obs}	d_{cal}	I/I_o	h	k	l	d_{obs}	d_{cal}	I/I_o	h	k	l
24.7999	24.8357	13.3	1	1	0	2.5079	2.5088	9.8	12	6	4
17.5445	17.5615	9.2	2	0	0	2.4974	2.4961	8.0	9	9	6
14.3023	14.3389	7.2	2	1	1	2.4837	2.4836	9.8	10	8	6
12.3976	12.4179	14.4	2	2	0	2.4591	2.4591	7.3	10	10	2
10.1200	10.1391	8.3	2	2	2	2.4476	2.4471	10.7	10	9	5
9.3886	9.3870	11.0	3	2	1	2.3894	2.3898	5.5	10	10	4
8.2773	8.2786	80.8	3	3	0	2.3784	2.3788	5.2	11	9	4
7.8569	7.8537	12.9	4	2	0	2.3572	2.3573	6.3	11	10	1
7.4909	7.4883	7.7	3	3	2	2.3475	2.3468	5.7	12	8	4
7.1694	7.1695	9.9	4	2	2	2.3358	2.3363	5.5	9	9	8
6.8886	6.8882	72.3	4	3	1	2.3160	2.3159	8.8	10	9	7
6.2090	6.2089	18.3	4	4	0	2.3061	2.3059	8.5	14	6	0
6.0204	6.0235	6.1	4	3	3	2.2963	2.2961	5.9	11	8	7
5.8539	5.8538	31.1	4	4	2	2.2863	2.2863	9.3	10	10	6
5.6980	5.6977	36.3	5	3	2	2.2579	2.2578	11.3	11	11	0
5.4203	5.4196	21.9	5	4	1	2.2490	2.2485	5.3	12	8	6
5.2958	5.2950	14.5	6	2	2	2.2395	2.2394	7.6	11	10	5
5.1798	5.1786	10.3	6	3	1	2.2216	2.2214	5.3	12	9	5
4.9672	4.9671	32.4	5	4	3	2.1949	2.1952	5.3	16	0	0
4.7799	4.7796	67.4	5	5	2	2.1875	2.1867	6.0	11	11	4
4.6942	4.6935	26.5	6	4	2	2.1784	2.1782	6.0	12	10	4
4.6125	4.6119	8.1	7	3	0	2.1702	2.1699	5.0	10	9	9
4.4605	4.4606	7.2	6	5	1	2.1546	2.1535	5.1	11	9	8
4.3908	4.3904	22.6	8	0	0	2.1448	2.1455	5.6	14	6	6
4.3236	4.3233	12.4	5	5	4	2.1379	2.1375	5.7	11	10	7
4.2594	4.2593	26.2	6	4	4	2.0696	2.0696	6.0	12	12	0
4.1992	4.1980	7.8	6	5	3	2.0625	2.0625	8.7	12	11	5
4.1378	4.1393	6.9	6	6	0	2.0486	2.0484	14.3	13	10	5
4.0834	4.0830	25.6	7	4	3	2.0341	2.0346	5.4	15	8	3
4.0303	4.0289	6.5	6	6	2	2.0144	2.0144	6.4	12	12	4
3.9743	3.9769	6.2	7	5	2	2.0080	2.0078	11.2	11	11	8
3.9269	3.9269	10.3	8	4	0	1.9887	1.9884	5.8	14	10	4
3.8790	3.8787	28.5	8	3	3	1.9697	1.9696	4.6	13	10	7
3.7866	3.7874	8.2	6	5	5	1.9572	1.9573	4.8	13	12	3
3.7026	3.7023	15.0	7	5	4	1.9453	1.9453	6.3	13	11	6
3.6214	3.6227	20.0	7	6	3	1.9396	1.9393	4.8	16	6	6
3.5844	3.5847	67.8	8	4	4	1.9219	1.9218	5.0	15	10	3
3.5476	3.5480	11.7	7	7	0	1.9107	1.9104	5.0	13	12	5
3.5128	3.5123	6.8	8	6	0	1.9046	1.9048	4.4	14	12	0
3.4445	3.4441	11.2	8	6	2	1.8877	1.8882	4.2	12	11	9
3.3789	3.3797	12.3	6	6	6	1.8773	1.8774	4.9	13	10	9
3.3488	3.3488	62.9	7	6	5	1.8669	1.8668	4.1	13	11	8
3.2614	3.2611	74.0	8	6	4	1.8461	1.8460	5.2	13	12	7
3.2342	3.2333	10.3	9	6	1	1.8346	1.8359	3.7	14	11	7
3.1800	3.1799	20.7	8	7	3	1.8260	1.8260	4.7	15	9	8
3.1291	3.1290	58.4	9	6	3	1.8158	1.8162	4.4	13	13	6
3.1055	3.1045	9.1	8	8	0	1.8114	1.8113	4.9	14	12	6
3.0806	3.0805	100.0	9	7	0	1.8068	1.8065	5.8	15	12	3
3.0345	3.0342	7.8	7	7	6	1.7741	1.7740	28.6	14	14	0
3.0107	3.0118	7.8	8	6	6	1.7649	1.7650	9.7	14	10	10
2.9901	2.9899	41.9	8	7	5	1.7563	1.7562	11.9	16	12	0
2.9676	2.9684	37.1	10	6	2	1.7476	1.7474	5.2	14	12	8
2.9466	2.9475	7.0	9	6	5	1.7347	1.7346	3.5	15	11	8

TABLE 3. (contd.)

d_{obs}	d_{cal}	I/I_o	h	k	l	d_{obs}	d_{cal}	I/I_o	h	k	l
2.9279	2.9269	6.2	8	8	4	1.7258	1.7262	3.7	14	13	7
2.9074	2.9068	10.3	9	7	4	1.7180	1.7179	6.0	15	12	7
2.8681	2.8678	14.2	10	5	5	1.7056	1.7057	4.1	18	8	6
2.8477	2.8489	12.1	10	6	4	1.7018	1.7017	3.8	16	11	7
2.8303	2.8303	10.3	9	8	3	1.6858	1.6860	4.5	13	12	11
2.7944	2.7942	14.0	10	7	3	1.6785	1.6782	7.7	13	13	10
2.7757	2.7767	6.8	12	4	0	1.6707	1.6706	9.0	17	12	3
2.7429	2.7426	9.0	8	8	6	1.6630	1.6631	7.0	14	13	9
2.7263	2.7261	39.1	9	7	6	1.6523	1.6520	3.5	16	14	0
2.7091	2.7098	8.4	10	8	2	1.6444	1.6448	5.7	14	14	8
2.6936	2.6938	6.1	9	8	5	1.6340	1.6341	5.7	17	13	2
2.6779	2.6781	6.1	10	6	6	1.6270	1.6270	6.6	15	15	4
2.6624	2.6627	7.0	10	7	5	1.6203	1.6201	4.2	15	14	7
2.6470	2.6475	6.4	12	4	4	1.6061	1.6065	3.3	19	9	6
2.6326	2.6326	18.5	9	9	4	1.5965	1.5965	6.3	14	12	12
2.6182	2.6179	46.4	10	8	4	1.5868	1.5867	8.2	15	12	11
2.6042	2.6035	8.5	10	9	1	1.5808	1.5803	3.6	15	13	10
2.5896	2.5893	5.7	12	6	2	1.5674	1.5676	4.4	15	14	9
2.5757	2.5753	14.6	11	7	4	1.5642	1.5645	4.4	18	12	6
2.5487	2.5481	6.7	10	9	3	1.5488	1.5492	4.5	15	15	8

the expected T–O value of 1.642(6) given in Jones (1968) for a Si/Al ratio of 3. The greatest mean bond length of ~1.65 Å is observed in the T1 tetrahedra, building a S6R between two π-cages and the T2 tetrahedra as a part of the semicircular 4-ring band. Using the ionic radius of oxygen given by Shannon (1976) for framework oxygens, the dynamic diameter of the main channel system (D8R [100]) and of the second diagonal pore system (S6R [111]) can be estimated to be ~4.25 Å and ~2.50 Å, respectively.

The location of the non-framework components

Three main cation positions (M1, M2, M3) with different chemical occupation preferences can be observed in the investigated paulingite. These locations are highly occupied and cover 82 of the 99 'heavy' Ca, K and Ba cations (Table 6), found by the chemical analysis. These main cation sites correspond to the locations of the unspecified electron densities given by Gordon et al. (1966) and to a short description of Bieniok and Baur (1996).

The position M1 is located in the centre of the π-cage and is fully occupied by Ca. This cation is surrounded by a coordination sphere of water molecules, which are bonded to the framework via hydrogen bonds. The possible positions of the water

molecules around the Ca ion are arranged in a slightly distorted cube, with a diagonal shortening along [111] between two fully occupied water
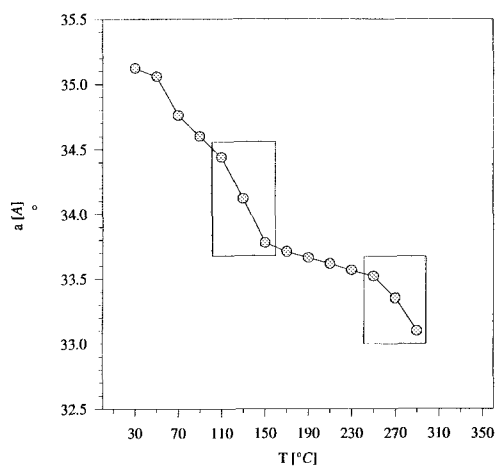
FIG. 4. The cell parameter evaluation of paulingite derived from the Guinier HT-measurement using the 2θ values of the (765), (864), and (972) reflections. The error of each data point is ±0.1 Å and ±5°C. The boxes indicate the temperature ranges with peak broadening.

C. L. LENGAUER *ET AL.*

TABLE 4. X-ray powder diffraction data of dehydrated paulingite from Vinaricá Hora

d_{obs}	d_{cal}	I/I_o	h	k	l	d_{obs}	d_{cal}	I/I_o	h	k	l
23.7927	23.8638	14.8	1	1	0	2.4110	2.4106	10.6	12	6	4
16.8851	16.8742	6.2	2	0	0	2.3992	2.3984	3.7	9	9	6
13.7761	13.7778	7.7	2	1	1	2.3741	2.3745	3.0	11	9	0
11.9238	11.9319	15.8	2	2	0	2.3611	2.3629	3.1	10	10	2
9.7312	9.7423	6.5	2	2	2	2.3528	2.3514	3.1	10	9	5
9.0240	9.0197	21.6	3	2	1	2.3288	2.3289	2.9	11	8	5
7.9566	7.9546	100.0	3	3	0	2.3066	2.3070	4.6	13	6	3
7.5414	7.5464	6.0	4	2	0	2.2964	2.2963	3.1	10	10	4
7.1871	7.1952	5.8	3	3	2	2.2852	2.2857	3.1	11	9	4
6.8852	6.8889	9.3	4	2	2	2.2650	2.2650	3.0	11	10	1
6.6208	6.6186	29.4	4	3	1	2.2348	2.2350	6.7	10	8	8
6.1566	6.1616	5.7	5	2	1	2.2153	2.2157	3.5	14	6	0
5.9682	5.9659	18.3	4	4	0	2.2061	2.2062	3.0	11	8	7
5.7850	5.7878	6.4	4	3	3	2.1969	2.1968	2.8	10	10	6
5.6226	5.6247	14.6	4	4	2	2.1698	2.1694	5.4	11	11	0
5.4762	5.4747	11.0	5	3	2	2.1517	2.1517	5.1	11	10	5
5.3362	5.3361	6.9	6	2	0	2.1334	2.1344	3.0	12	9	5
5.2113	5.2075	7.1	5	4	1	2.1177	2.1176	2.7	13	7	6
5.0834	5.0878	5.6	6	2	2	2.1097	2.1093	2.6	16	0	0
4.9792	4.9759	5.3	6	3	1	2.1006	2.1011	2.7	11	11	4
4.8639	4.8712	5.3	4	4	4	2.0930	2.0930	2.9	12	10	4
4.7737	4.7728	19.1	5	4	3	2.0769	2.0771	2.8	10	10	8
4.5937	4.5926	21.0	5	5	2	2.0698	2.0693	2.9	11	9	8
4.5119	4.5098	8.3	6	4	2	2.0612	2.0615	3.7	14	6	6
4.2833	4.2861	6.4	6	5	1	2.0524	2.0539	2.9	11	10	7
4.2197	4.2186	14.9	8	0	0	2.0391	2.0388	2.7	12	9	7
4.1554	4.1542	5.5	5	5	4	2.0245	2.0241	2.8	11	11	6
4.0936	4.0926	12.1	6	4	4	2.0093	2.0097	2.6	13	8	7
4.0360	4.0337	6.0	6	5	3	1.9876	1.9886	2.7	12	12	0
3.9779	3.9773	4.9	6	6	0	1.9822	1.9818	3.0	12	11	5
3.9244	3.9232	10.8	7	4	3	1.9685	1.9683	3.2	13	10	5
3.8734	3.8712	4.7	6	6	2	1.9414	1.9420	2.5	11	10	9
3.8243	3.8213	4.6	7	5	2	1.9296	1.9293	3.7	11	11	8
3.7279	3.7269	14.2	8	3	3	1.9107	1.9106	4.4	14	10	4
3.6805	3.6823	4.9	8	4	2	1.8759	1.8749	3.1	12	12	6
3.6393	3.6392	7.7	6	5	5	1.8699	1.8692	3.8	13	11	6
3.5941	3.5976	5.4	6	6	4	1.8467	1.8466	3.7	15	10	3
3.5576	3.5574	13.6	7	5	4	1.8359	1.8357	2.7	13	12	5
3.4811	3.4809	11.0	7	6	3	1.8244	1.8249	2.2	11	11	10
3.4451	3.4444	15.3	8	4	4	1.8041	1.8039	3.1	13	10	9
3.4095	3.4091	6.5	7	7	0	1.7944	1.7937	2.2	13	11	8
3.3759	3.3748	4.3	8	6	0	1.7834	1.7837	2.3	14	9	9
3.3430	3.3416	4.6	7	7	2	1.7741	1.7738	2.8	13	12	7
3.3058	3.3093	4.3	8	6	2	1.7546	1.7545	2.3	15	9	8
3.2767	3.2779	4.6	9	4	3	1.7452	1.7451	2.4	13	13	6
3.2476	3.2474	12.9	6	6	6	1.7403	1.7404	2.7	14	12	6
3.2183	3.2178	31.1	7	6	5	1.7362	1.7358	2.9	15	12	3
3.1608	3.1608	5.2	7	7	4	1.7172	1.7178	2.2	12	11	11
3.1340	3.1335	27.8	8	6	4	1.7080	1.7089	3.1	13	11	10
3.1060	3.1068	4.6	9	6	1	1.7041	1.7046	3.1	14	14	0
3.0824	3.0808	4.2	10	4	2	1.6963	1.6959	2.3	14	10	10
3.0551	3.0554	6.1	8	7	3	1.6875	1.6874	3.3	16	12	0
3.0070	3.0066	14.3	9	6	3	1.6796	1.6790	2.6	14	12	8

TABLE 4. (contd.)

d_{obs}	d_{cal}	I/I_o	h	k	l	d_{obs}	d_{cal}	I/I_o	h	k	l
2.9604	2.9599	27.7	9	7	0	1.6670	1.6667	3.4	15	11	8
2.9353	2.9374	4.3	8	8	2	1.6585	1.6586	2.7	14	13	7
2.9156	2.9154	8.1	7	7	6	1.6503	1.6507	2.3	15	12	7
2.8734	2.8729	14.5	8	7	5	1.6382	1.6390	2.5	18	8	6
2.8526	2.8523	5.2	10	6	2	1.6352	1.6351	2.6	16	11	7
2.7937	2.7930	4.7	9	7	4	1.6199	1.6200	2.6	13	12	11
2.7552	2.7556	5.8	10	5	5	1.6129	1.6126	3.0	13	13	10
2.7368	2.7374	6.1	10	6	4	1.6049	1.6053	2.9	17	12	3
2.7202	2.7195	6.4	9	8	3	1.5981	1.5980	3.3	14	13	9
2.6854	2.6849	3.8	10	7	3	1.5901	1.5909	2.9	15	12	9
2.6513	2.6515	5.8	8	7	7	1.5807	1.5804	2.9	14	14	8
2.6353	2.6353	4.4	8	8	6	1.5709	1.5701	2.0	17	13	2
2.6197	2.6194	9.3	9	7	6	1.5628	1.5634	2.4	15	15	4
2.6038	2.6038	3.9	10	8	2	1.5561	1.5567	2.6	15	14	7
2.5585	2.5585	5.7	10	7	5	1.5510	1.5501	2.3	16	13	7
2.5299	2.5296	4.8	9	9	4	1.5431	1.5436	2.5	19	9	6
2.5159	2.5155	7.8	10	8	4	1.5343	1.5340	2.9	14	12	12
2.5001	2.5016	4.0	10	9	1	1.5251	1.5246	3.9	15	12	11
2.4751	2.4746	4.7	11	7	4	1.5183	1.5184	2.8	15	13	10
2.4483	2.4484	2.8	10	9	3	1.5060	1.5063	2.7	15	14	9
2.4229	2.4230	5.2	9	8	7	1.5004	1.5003	2.3	16	13	9

positions (W1, W2) and an elongation towards six half occupied water positions (W6, W7) oriented to the 8-rings of the cage (Fig. 5a). The W6—W7 distance is 2.58(2) Å.

The Ba position (M2) is situated in the centre of the opening of the semicircular band of the five 4-rings between two adjacent 8-rings of neighbouring π-cages (Fig. 5b). Based on the electron density of the difference Fourier maps and the observed chemical formula the refinement reveals a ¾ occupancy by Ba. The coordination sphere of this cation position consists of a tetrahedral surrounding of four water molecules (W3 s.o.f. 1, W8 s.o.f. ¾), and additional bondings to six framework oxygens (3 × O3, 3 × O17).

Taking into account chemical constraints, electron density and displacement factors, the third pronounced cation position (M3) is expected to be occupied by K (75%) and minor amounts of Ca (15%) and Ba (10%). This crystallographic site is in the centre of the nonplanar 8-ring of the γ-cage, and is known to be preferred by K in zeolite ZK-5 (Fischer, 1990). The cations are therefore coordinated by the six nearest framework oxygens (2 × O14, 2 × O15, 2 × O16), and by two water molecules (W4 s.o.f. 1, W5 s.o.f. ¾) inside the semicircular band of five 4-rings attached to the

γ-cage (Fig. 5c). A further bonding (M3—O: ~2.7 Å) can be observed in the 1/4-occupied position W15, which is part of the water cluster inside the γ-cage.

The remaining alkali and alkaline-earth pore filling can be distributed over partially occupied positions, either located in the centre of the planar 8-rings of the main channel system (M12, M13), or between two γ-cages outside of the D8R (M9). All three possible cation-sites are bonded to partially occupied positions of water molecules inside the α- (M12) and the γ-cages (M13), or to a surrounding of a water cluster (M9). Using the same restrictions as for M3 a storing of Ca on the sites M12 and M9, and of Na on the site M13 gave reliable refinement results with respect to chemistry and displacement factors.

The positions of the water molecules within the paulingite pore system, which are not distinctly bonded to the main cations M1—3, can be divided into three independent cluster configurations of partially occupied sites (Table 6). The water cluster inside the γ-cage, which is based on the four crystallographic sites W14, W15, W20 and W24, and fills the space between the cation site M13 in the centre of the planar 8-ring as a part of the D8R of the main channel and the K site M3 in the centre of the non-planar 8-ring. The respective site occupancies are from 25 to 50%. The arrangement of the water

TABLE 5. Structural parameters of the framework sites of paulingite from Vinarická Hora

	$W^{(i)}$	$m^{(ii)}$	x	y	z	$U_{eq}^{(iii)}$	U_{11}	U_{22}	U_{33}	U_{23}	U_{13}	U_{12}
T1$^{(iv)}$	i	48	0.31415(4)	0.25	$0.5-x$	0.0154(5)	0.0152(7)	0.016(1)	U_{11}	0.0011(7)	0.0025(9)	U_{23}
T2	i	48	0.40239(4)	0.25	$0.5-x$	0.0168(5)	0.0164(7)	0.018(1)	U_{11}	−0.0021(7)	0.002(1)	U_{23}
T3	l	96	0.31326(4)	0.24994(4)	0.09777(5)	0.0164(4)	0.0149(9)	0.0190(9)	0.0152(8)	−0.0033(7)	−0.0009(7)	0.0024(7)
T4	l	96	0.45599(5)	0.10747(4)	0.04451(5)	0.0182(4)	0.0193(8)	0.0183(8)	0.0169(8)	0.0028(7)	−0.0003(7)	0.0054(7)
T5	l	96	0.40182(4)	0.17831(5)	0.04459(5)	0.0175(4)	0.0163(8)	0.0180(8)	0.0183(8)	−0.0029(7)	−0.0025(7)	0.0024(7)
T6	l	96	0.31241(4)	0.17825(4)	0.04496(5)	0.0164(3)	0.0167(8)	0.0187(8)	0.0138(8)	−0.0008(7)	0.0012(7)	−0.0031(7)
T7	l	96	0.25946(4)	0.10767(4)	0.04451(4)	0.0149(3)	0.0144(7)	0.0161(8)	0.0141(8)	0.0029(7)	−0.0003(7)	−0.0022(6)
T8	l	96	0.17112(4)	0.10769(4)	0.04405(5)	0.0168(4)	0.0160(8)	0.0182(8)	0.0161(8)	0.0034(7)	0.0016(7)	0.0047(7)
O1	j	48	0.1634(2)	0.0938(2)	0	0.029(1)	0.030(4)	0.029(3)	0.028(3)	0	0	0.000(3)
O2	j	48	0.2683(2)	0.0969(2)	0	0.026(1)	0.030(3)	0.029(3)	0.018(3)	0	0	0.003(3)
O3	j	48	0.3031(2)	0.1878(2)	0	0.025(1)	0.029(3)	0.030(3)	0.016(3)	0	0	0.002(3)
O4	j	48	0.4087(2)	0.1898(2)	0	0.038(2)	0.052(4)	0.036(4)	0.025(3)	0	0	−0.011(3)
O5	j	48	0.4490(2)	0.0962(2)	0	0.035(2)	0.032(4)	0.046(4)	0.028(3)	0	0	−0.003(3)
O6	j	48	0.4493(2)	0.3786(2)	0	0.030(2)	0.034(4)	0.026(3)	0.029(3)	0	0	0.002(3)
O7	k	48	0.0716(1)	x	0.1613(2)	0.032(2)	0.032(2)	U_{11}	0.030(3)	0.000(2)	U_{23}	0.009(3)
O8	k	48	0.4303(1)	x	0.2315(2)	0.033(2)	0.032(2)	U_{11}	0.034(4)	0.006(2)	U_{23}	0.014(3)
O9	k	48	0.1439(1)	x	0.0547(2)	0.029(2)	0.026(2)	U_{11}	0.034(4)	−0.001(2)	U_{23}	0.009(3)
O10	k	48	0.2860(1)	x	0.1961(2)	0.034(2)	0.031(2)	U_{11}	0.039(4)	−0.004(2)	U_{23}	0.008(3)
O11	k	48	0.2879(1)	x	0.0888(2)	0.036(2)	0.036(2)	U_{11}	0.037(4)	0.008(2)	U_{23}	0.009(3)
O12	k	48	0.4302(1)	x	0.0536(2)	0.037(2)	0.035(2)	U_{11}	0.040(4)	−0.004(2)	U_{23}	0.016(3)
O13	l	96	0.2153(1)	0.1223(1)	0.0498(1)	0.027(1)	0.021(2)	0.029(2)	0.030(2)	0.002(2)	0.002(2)	0.004(2)
O14	l	96	0.2878(1)	0.1413(1)	0.0592(1)	0.034(1)	0.035(3)	0.042(3)	0.025(2)	−0.003(2)	0.002(2)	−0.019(2)
O15	l	96	0.3573(1)	0.1681(1)	0.0528(1)	0.033(1)	0.027(2)	0.038(3)	0.034(3)	0.006(2)	−0.001(2)	0.000(2)
O16	l	96	0.4268(1)	0.1411(1)	0.0572(1)	0.040(1)	0.039(3)	0.039(3)	0.041(3)	0.003(2)	0.000(2)	0.022(2)
O17	l	96	0.2997(1)	0.2163(1)	0.0685(1)	0.034(1)	0.035(3)	0.033(3)	0.035(3)	−0.014(2)	0.004(2)	−0.004(2)
O18	l	96	0.4156(1)	0.2141(1)	0.0706(1)	0.034(1)	0.033(3)	0.029(2)	0.040(3)	−0.015(2)	−0.001(2)	−0.002(2)
O19	l	96	0.3575(1)	0.2617(1)	0.0902(1)	0.031(1)	0.027(2)	0.034(3)	0.032(2)	0.007(2)	−0.001(2)	−0.002(2)
O20	l	96	0.3075(1)	0.2355(1)	0.1417(1)	0.026(1)	0.034(2)	0.025(2)	0.020(2)	0.006(2)	0.002(2)	−0.003(2)

The e.s.d.s are given in parentheses, and the elements of the anisotropic displacement factor are defined as $\exp[-2\pi^2 \Sigma_i \Sigma_j U_{ij} h_i h_j a_i^* a_j^*]$. [i]Wyckoff letter, [ii]atoms per cell, [iii]the equivalent isotropic displacement factor $U_{eq} = 1/3\ \Sigma_i \Sigma_j U_{ij} a_i^* a_j^* a_i a_j$ (Fischer and Tillmanns, 1988), [iv]T = 0.73 Si + 0.27 Al.

TABLE 6. Structural parameters of the non framework sites of paulingite from Vinaricka Hora

	W[i]	m[ii]	s.o.[iii]	x	y	z	$U_{eq/iso}$
M1	f	16	16 Ca	0.17896(6)	x	x	0.0379(9) U_{eq}
M2	h	24	18 Ba	0.25711(3)	x	0	0.0494(4) U_{eq}
M3	k	48	36 K, 7 Ca, 5 Ba	0.39865(4)	x	0.14379(6)	0.0498(5) U_{eq}
M9	j	48	9 Ca	0.4191(8)	0.2874(7)	0	0.15(1)
M12	e	12	4 Ca	0.175(1)	0	0	0.15[iv]
M13	e	12	5 Na	0.257(1)	0	0	0.15[iv]
W1	f	16	16 H_2O	0.1408(3)	x	x	0.086(6)
W2	f	16	16 H_2O	0.2176(3)	x	x	0.088(5)
W3	k	48	48 H_2O	0.2082(2)	x	0.0500(2)	0.071(2)
W4	k	48	48 H_2O	0.3500(2)	x	0.1968(3)	0.077(3)
W5	k	48	36 H_2O	0.3518(2)	x	0.0919(4)	0.075(3)
W6	k	48	24 H_2O	0.2156(4)	x	0.1324(6)	0.097(7)
W7	k	48	24 H_2O	0.1433(4)	x	0.2226(6)	0.091(7)
W8	j	48	36 H_2O	0.3369(4)	0.2737(4)	0	0.085(4)
W14	e	12	4 H_2O	0.410(3)	0	0	0.19(2)
W15	l	96	24 H_2O	0.464(1)	0.433(1)	0.143(1)	0.19[v]
W20	e	12	6 H_2O	0.455(2)	0	0	0.19[v]
W24	j	48	14 H_2O	0.311(2)	0.030(1)	0	0.19[v]
W17	f	16	4 H_2O	0.0613(14)	x	x	0.109(5)
W22	k	48	5 H_2O	0.0270(4)	x	0.1224(6)	0.109[vi]
W23	h	24	3 H_2O	0.0302(24)	x	0	0.109[vi]
W10	g	24	8 H_2O	0.2992(14)	0.5	0	0.109[vi]
W11	h	24	10 H_2O	0.3592(8)	x	0	0.109[vi]
W16	l	96	38 H_2O	0.4553(5)	0.2465(6)	0.0204(5)	0.109[vi]
W19	j	48	17 H_2O	0.4544(11)	0.2845(10)	0	0.109[vi]
W21	l	96	15 H_2O	0.3248(14)	0.3856(15)	0.0289(14)	0.109[vi]

The e.s.d.s are given in parentheses, and the equivalent isotropic displacement factor $U_{eq} = 1/3 \ \Sigma_i \Sigma_j U_{ij} a_i^* a_j^* a_i a_j$ is calculated according to Fischer and Tillmanns (1988).The atoms are labelled after Gordon *et al.* (1966). [i]Wyckoff letter, [ii]atoms per cell, [iii]chemical site occupation of the refinement, [iv]constrained to be equal to U_{iso} of M9, [v]constrained to be equal to U_{iso} of W14, [vi]constrained to be equal to U_{iso} of W17.

molecules inside the α-cage exhibits a weak bonding of the whole cluster to the cation-site M12 in the centre of the planar 8-ring. The cluster itself is built by three locations of water molecules (W17, W22, W23) refined to occupancies of 10–25%. The distance M12–W22 is 2.36(3) Å. The third water concentration within the paulingite structure is a bonding sphere around cation-site M9 outside the D8R. It is established by the sites W10, W16, W19, W21, which can be refined to occupancies of 15 to 40%.

The structural role of the water content

As pointed out in the description of the thermal behaviour, the main ˉweight loss in the range 24–190°C is accompanied by a remarkable 11% reduction of the paulingite cell volume without a change in the characteristics of the framework. The minor second weight loss in the range 190–390°C, however, leads to a breakdown of the paulingite structure. The calculated water content of this second step is ~6H_2O molecules per formula unit, which is in the range of the distorted water-cube around the M1 site (Ca) inside the π-cage (5H_2O p.f.u.). Therefore one can conclude that the main weight loss with its maximum at 70°C is caused mainly by a decomposition of the water clusters inside the α-cage and γ-cages via the main channel system with its larger dynamic diameter of ~4.25 Å. The H_2O-desorption from these large polyhedral units is likely to be the reason for the observed shrinkage of the paulingite

TABLE 7. Selected interatomic bond lengths [Å] and angles [°] of paulingite from Vinaricka Hora

Framework Cations

T1–O10	2×	1.645(4)	O–T1–O	107.2(2)–111.4(2)	M1–W1		2.32(1)
T1–O20	2×	1.652(4)	T1–O10–T1	151.1(4)	M1–W2		2.35(1)
\<T1–O\>		1.649(4)	T1–O20–T3	0.4(3)	M1–W7	3×	2.34(1)
					M1–W6	3×	2.45(1)
T2–O18	2×	1.645(4)	O–T2–O	105.6(2)–111.6(2)	\<M1–W\>		2.38
T2–O19	2×	1.651(4)	T2–O18–T5	146.5(3)			
\<T2–O\>		1.648(3)					
T3–O19		1.631(4)	O–T1–O	106.4(2)–111.6(3)	M2–W8	2×	2.86(1)
T3–O11		1.634(5)	T3–O11–T3	148.7(3)	M2–O3	2×	2.922(6)
T3–O17		1.635(4)	T3–O19–T2	145.0(3)	M2–W3	2×	3.00(1)
T3–O20		1.638(4)			M2–O17	4×	3.178(4)
\<T3–O\>		1.635(3)			\<M2–O/W\>		3.03
T4–O16		1.629(4)	O–T4–O	106.9(2)–111.6(2)	M3–W15		2.59(5)
T4–O12		1.629(5)	T4–O5–T4	146.3(4)	M3–O15	2×	2.899(5)
T4–O5		1.633(2)	T4–O6–T4	141.7(3)	M3–W5		2.96(1)
T4–O6		1.637(6)	T4–O12–T4	147.4(4)	M3–W4		3.05(1)
\<T4–O\>		1.632(4)	T4–O16–T5	147.5(3)	M3–O14	2×	3.153(5)
					M3–O16	2×	3.240(5)
T5–O18		1.625(4)	O–T5–O	107.8(2)–112.0(2)	\<M3–O/W\>		3.02
T5–O15		1.629(4)	T5–O4–T5	146.7(4)			
T5–O16		1.633(2)	T5–O15–T6	147.4(3)			
T5–O4		1.635(2)					
\<T5–O\>		1.631(4)					
T6–O17		1.632(4)	O–T6–O	105.8(2)–113.1(2)	M9–W21		3.03(5)
T6–O14		1.639(4)	T6–O3–T6	147.3(4)	M9–W16		2.05(3)
T6–O15		1.643(4)	T6–O17–T3	146.3(3)	M9–W10		2.87(6)
T6–O3		1.646(2)			M9–W8		2.93(3)
\<T6–O\>		1.640(6)			M9–O18	2×	2.987(6)
					M9–W11		3.28(4)
T7–O14		1.628(4)	O–T7–O	107.2(2)–112.1(2)			
T7–O8		1.631(5)	T7–O2–T7	145.5(4)	M12–W22		2.28(3)
T7–O2		1.637(2)	T7–O8–T7	148.1(3)	M12–O1	4×	3.320(7)
T7–O13		1.646(6)	T7–O14–T6	143.1(3)	M12–O7	4×	3.590(7)
\<T7–O\>		1.636(8)					
					M13–W24		2.17(7)
T8–O7		1.632(5)	O–T8–O	106.5(2)–111.7(2)	M13–O2	4×	3.427(8)
T8–O9		1.636(4)	T8–O1–T8	140.4(4)	M13–O8	4×	3.485(8)
T8–O13		1.640(4)	T8–O7–T8	151.0(3)			
T8–O1		1.644(2)	T8–O9–T8	149.0(4)			
\<T8–O\>		1.638(5)	T8–O13–T7	141.3(2)			

framework, a structural behaviour also known from the zeolite, erionite (Schlenker *et al.*, 1977). The bonding of the Ca-$(H_2O)_6$ polyhedra, supported by the charge compensation of the low Si/Al ratio and its encapsulation in the π-cage (dynamic diameter: ~2.50 Å), might prevent a decomposition below 190°C, and can be interpreted as acting as a structure stabilizing template within the paulingite pore system at elevated temperatures.

Besides that, one has to note, that the refined cell parameter for the paulingite of Vinaricka Hora exhibits the largest value found up to now for paulingite, which is in contradiction to the obviously low water content and its expected lowering of the cell parameter. The value, however, is in accordance with the observed low Si/Al-ratio and suggests that even structures with a low framework density can compensate for a limited loss of pore filling.
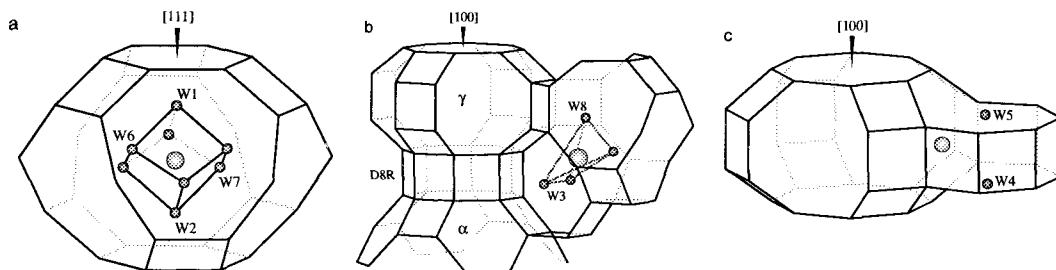
FIG. 5. (a) The cation site M1 (Ca) surrounded by water molecules inside the tetrahedral framework of the π-cage; (b) the cation of the M2 site (Ba) surrounded by a tetrahedron of water molecules plus six additional bondings to framework oxygens; (c) the cation site M3 (K) in the centre of the nonplanar 8-ring of the γ-cage and the two water molecules in the semicircular band of the five 4-rings attached to the γ-cage. The tetrahedral framework is indicated by solid lines representing the T−T bonds, the cations are shown as big (light grey), the water molecules as small (dark grey) balls, respectively.

References

Andersson, S. and Fälth, L. (1983) An alternative description of the paulingite structure. *J. Solid State Chem.*, **46**, 265−8.

Appleman, D.E. and Evans, H.T. (1973) Indexing and least-squares refinement of powder diffraction data., *U.S. Geol. Surv. Comp. Contrib.*, **20**, PB2-16188.

Bieniok, A. and Baur, W.H. (1996) Strukturelle Variationen des Zeoliths Paulingit. *Z. Kristallogr.*, Supplement Issue No. **11**, 112.

Efremov, N. (1951) Neuigkeiten aus den mineralogischen Untersuchungen der Ukraine und Rußlands. *Fortschr. Mineral.*, **29-30**, 84−6.

Fischer, R.X. and Tillmanns, E. (1988) The equivalent isotropic displacement factor. *Acta Crystallogr.*, **C44**, 775−6.

Fischer, R.X. (1990) *Der Zeolith ZK-5: Von der K,Cs-Modifikation zum Katalysator.* Habilitationsschrift, Universität Würzburg, FRG.

Gordon, K.E., Samson, S. and Kamb, W.B. (1966) Crystal structure of the zeolite paulingite. *Science*, **154**, 1004−7.

Gottardi, G. and Galli, E. (1985) *Natural Zeolites.* Springer, Berlin Heidelberg, 164−7.

Hawthorne, F.C. and Smith, J.V. (1986) Enumeration of 4-connected 3-dimensional nets and the classification of framework silicates: body centered cubic nets based on the rhombicuboctahedron. *Canad. Mineral.*, **24**, 643−8.

Hentschel, G. (1986) Paulingit und andere seltene Zeolithe in einem gefritteten Sandsteineinschluß im Basalt von Ortenberg (Vogelsberg). *Geol. Jahrb. Hessen.*, **114**, 249−56.

Hlouek, J., Veselovsk, F. and Rychl R. (1988) Chemismus paulingitu z Vinarické hory. *Casopis pro mineralogii a geologii*, **33**, 109.

Jones, J.B. (1968) Al-O and Si-O tetrahedral distances in aluminosilicate framework structures. *Acta Cryst.*, **B24**, 355−8.

Katzer, F. (1892) *Geologie von Böhmen.* I. Taussig, Praha, 1405−6.

Kamb, W.B. and Oke, W.C. (1960) Paulingite, a new zeolite, in association with erionite and filiform pyrite. *Amer. Mineral.*, **45**, 79−91.

Mandarino, J.A. (1981) The Gladstone-Dale relationship: part IV. The compatibility concept and its application. *Canad. Mineral.*, **19**, 441−50.

Meier, W.M. and Kokotailo, G.T. (1965) The crystal structure of synthetic zeolite ZK-5. *Z. Kristallogr.*, **121**, 211−9.

Meier, W.M., Olson, D.H. and Baerlocher, Ch. (1996): Atlas of zeolite structure types, 4th edition. *Zeolites*, **17**, 1−230.

Nawaz, R. (1988) A note on occurrence and optical orientation of brewsterite. *Mineral. Mag.*, **52**, 416−7.

Rouse, R.C., Peacor, R.D. and Merlino S. (1989) Crystal structure of pahasapaite,a beryllophosphate mineral with a distorted zeolite rho framework. *Amer. Mineral.*, **74**, 1195−202.

Schlenker, J.L., Pluth, J.J., Smith, J.V. (1977): Dehydrated natural erionite with stacking faults of the offretite type. *Acta Crystallogr.*, **B33**, 3265−8.

Shannon, R.D. (1976) Revised effective ionic radii and systematic studies of interatomic distances in halides and chalcogenides. *Acta Crystallogr.*, **A32**, 751–67.

Sheldrick, G.M. (1996) *SHELXL-96 Program for crystal structure refinement.* Universität Göttingen, FRG.

Smith, G.S. and Snyder, R.L. (1979) F_N: A criterion for rating powder diffraction patterns and evaluating the reliability of powder pattern indexing. *J. Appl. Crystallogr.*, **12**, 60–5.

Speckels, M.L. (1991) Microminerals at Rock Island Dam, Douglas County, Washington. *Rocks and Minerals*, **66**, 226–31.

Suk, M. (1984) *Geological history of the territory of the Czech Socialist Republic.* Academia Press, Praha, pp. 1–256.

Treacy, M.M., Higgins, J.B. and Ballmoos, R.v. (1996) Collection of simulated XRD powder patterns for zeolites. *Zeolites*, **16**, 327–802.

Tschernich, R.W. and Wise, W.S. (1982) Paulingite: variations in composition. *Amer. Mineral.*, **67**, 799–803.

Tschernich, R.W. (1992) *Zeolites of the World.* Geoscience Press Inc., Phoenix, Arizona, 396–400.

Vaughan, D.E.W. and Strohmaier, K.G. (1987) Zeolite (ECR-18) isostructural with paulingite and a method for its preparation. U.S. Patent Number 4,661,332.

Walenta, K., Zwiener, M. and Telle, R. (1981) Seltene Mineralien aus dem Nephilinit-Steinbruch am Höwenegg im Hegau: Makatit und Paulingit. *Der Aufschluß*, **25**, 130–4.